Investigation of the JT-60SA operation scenarios combined with integrated real-time controls

T. Suzuki[1], N. Hayashi[1], H. Urano[1], Y. Miyata[1], M. Honda[1], S. Ide[1] and the JT-60SA Team

[1] *Japan Atomic Energy Agency, Naka, Japan*

1. Introduction

The JT-60SA experiment program [1] aims at supporting ITER and providing the physics basis for DEMO having a broad conceptual/design spectrum, and hence, paves the way for the early realization of a fusion reactor. Especially, JT-60SA explores steady-state operation regime in high beta [2] complementing ITER. In the steady-state operation, real-time control of plasma parameters is essential in avoiding MHD activities and sustaining the plasma at high performance within the machine capability. Since such high beta plasma has large bootstrap current, the plasma exhibits non-linear nature arising from the coupling between pressure and current profiles through the bootstrap current. Necessary and sufficient control of the plasma with large bootstrap current fraction f_{BS} is not fully recognized so that it must be established in JT-60SA. We have started numerically investigating the steady-state operation prior to the experiment, implementing real-time control capability as well as a controller in 1.5D transport code TOPICS. We report here the operation scenarios realized using the real-time control in JT-60SA.

2. Plasma model in the TOPICS simulation, heating and current drive systems in JT-60SA and control scheme implemented in the TOPICS code

The TOPICS code solves current diffusion and core thermal transport while density profile and edge temperature profile are prescribed and fixed in this study. We assume the controlled plasma is in ELMy H-mode so that the density and temperature profiles have pedestals. Regarding the thermal transport, the CDBM anomalous transport model [3] is added to the neo-classical one. Impurity is carbon and effective charge is assumed as 2 (spatially uniform). Pedestal temperature (r/a=0.8-1) is prescribed to give H_H=1 after a TOPICS simulation in prescribed density profile without ITB at moderate power (β_N~2, without ITB in temperature profile) in monotonic safety factor (q) profile.

Regarding actuators, figure 1 shows the heating and current drive systems in JT-60SA. There are N-NB (500 keV, 10 MW by 2 ion-sources, co-I_p direction in off-axis), tangential

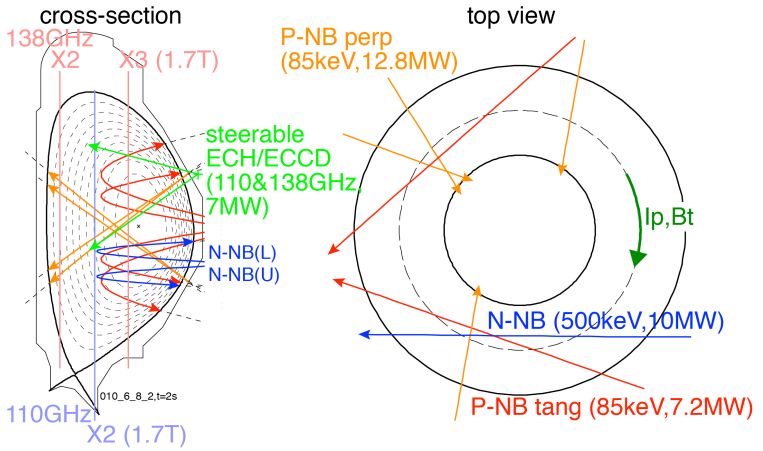

Fig. 1: Heating and current drive systems in JT-60SA in cross-sectional view and top view. Resonance surfaces for cold plasma at B_t=1.7 T are shown as well. The plasma configuration is the same as what is used in this study.

P-NB (85 keV, 7.2 MW by 8 ion-sources, 4 co- and 4 counter-I_p direction), perpendicular P-NB (85 keV, 12.8 MW by 16 ion-sources), and ECRH (7 MW into torus by 9 110/138 GHz-dual-frequency gyrotrons with toroidally and poloidally steerable antennae). The power is in the integrated research phase and total 37MW is available for heating.

In order to achieve the steady-state high beta plasma, onset of an MHD activity is a concern. Although JT-60SA is designed to stabilize MHD modes (e.g. RWM and NTM) by some tools (e.g. segmented in-vessel coils and ECRH, respectively), unlimited increase in beta will result in the onset of an MHD activity. Thus, we control β_N as an index of the MHD stability limit. Another concern in the steady-state operation is the loop voltage (V_{loop}). If the V_{loop} is non-zero and uncontrolled, Ohmic coil currents continue to change (at fixed I_p basically assumed), which results in stop of the operation at coil current limit. Since we think these two parameters (β_N and V_{loop}) are the essential ones to be controlled at least, we designed a controller and implemented it in the TOPICS code. Heating and current drive (CD) power can control β_N and V_{loop}, respectively, while the CD power is a part of the heating power.

Assuming plasma response be linearized around a specified operation point, as a first step, we selected PID control scheme (I-controller being RC-type integrator with a specified time constant τ_I) in a matrix form for multi-input multi-output (MIMO) control:

$$\begin{pmatrix} P_1(t+dt) \\ P_2(t+dt) \\ \vdots \end{pmatrix} = \begin{pmatrix} \mathrm{PID}_{11} & \mathrm{PID}_{12} & \cdots \\ \mathrm{PID}_{21} & \mathrm{PID}_{22} & \cdots \\ \vdots & \vdots & \ddots \end{pmatrix} \begin{pmatrix} \beta_{\mathrm{Nref}}(t) - \beta_N(t) \\ V_{\mathrm{loop\ ref}}(t) - V_{\mathrm{loop}}(t) \\ \vdots \end{pmatrix}$$

Coupling between the controlled parameters can be taken into account and this controller is extendable for other purposes in future. In this study, we allocated P-NB (both tangential and perpendicular) and EC (perpendicular injection to toroidal field) heating to P_1 (27 MW max in total) and N-NB CD to P_2 (5 MW + 5 MW).

In the control scheme, we implemented control cycle (dt_{cycle}) and delay time of actuator ON and OFF after commands (dt_{delay_ON}, dt_{delay_OFF}). We used dt_{cycle}=10 ms, dt_{delay_ON}=40 ms and dt_{delay_OFF}=0 ms, as the base parameters here.

3. Real-time control of normalized beta and loop voltage in JT-60SA

First of all, P-controls (or I-control with a short time constant for smoothing purpose) are employed here and the control gains are optimized through their scans. With increasing the gain, residual between the reference and the controlled parameter becomes smaller while modulation amplitude of the allocated power becomes larger. From a trade-off between them, we have determined the gains as follows; $G_{P\beta}$=400 MW, $G_{I\beta}$=400 MW/s, $\tau_{I\beta}$=0.5 s, G_{IV}=-2500 MW/V/s, τ_{IV}=0.2 s. Note that aforementioned parameters (dt_{cycle} and dt_{delay_ON}) can change the dynamics of the control systems as well: shorter control cycle reduces both the residual and modulation amplitude while shorter actuator delay reduces residual only.

As the steady-state operation scenario to be developed using the real-time control system, we selected I_p=2.3 MA and B_t=1.7 T at q_{95}=5.6, where plasma shape is shown in Fig. 1. We use ECRF as X3 scheme for ECH at r/a~0.2 here. Figure 2 shows waveforms of the real-time control of β_N and V_{loop} at line averaged electron density normalized to Greenwald density limit f_{GW}=0.88. The prescribed n_e profile is shown in Fig. 3 (a). The control starts at t=0 s and continues for 50 s. Reference of β_N is raised by 3 steps (3, 4 and 4.2) with time and β_N follows well its reference. Reference of V_{loop} is set to zero during the control and V_{loop}~0 is achieved during β_N=4, when power modulation in one of the two N-NB starts at t~21 s. Small residual (~0.01 V) between the V_{loop} and its reference remains because the V_{loop} control employs only I-control with a short time constant. After β_N being raised to 4.2, heating power controlling β_N increases and N-NB power controlling V_{loop} decreases (see the duty of N-NB). Control margin of heating power seems narrow in this phase. Figure 3 shows profiles of pressure and current related quantities. Reversed magnetic shear is sustained by the off-axis N-NBCD driven current and the bootstrap current and produces strong ITB in both electrons and ions through the CDBM model [3]. During V_{loop}~0 period, f_{BS} is 0.63-0.68.

Controllability of β_N and V_{loop} is investigated at distinct lower density regime at f_{GW}=0.52. Prescribed n_e profile in Fig. 3 (a) is now multiplied by 1/1.7, and instead, prescribed pedestal temperatures (r/a=0.8-1 in Fig. 3 (b) and (d)) are multiplied by 1.5 to obtain H_H=1 without n_e ITB. Figure 4 shows the result of the control. Also at this low

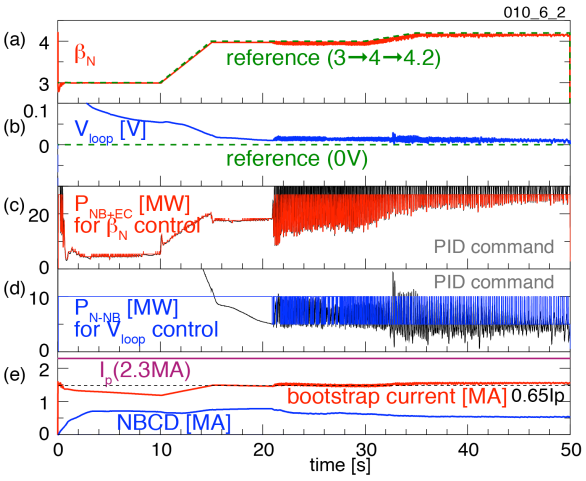

Fig. 2: Real-time control of β_N and V_{loop} at high density f_{GW}=0.88. (a) β_N and reference, (b) V_{loop} and reference, (c) P-NB and ECRF heating power controlling β_N, (d) N-NB current drive power controlling V_{loop}, (e) plasma current, bootstrap current and NBCD current.

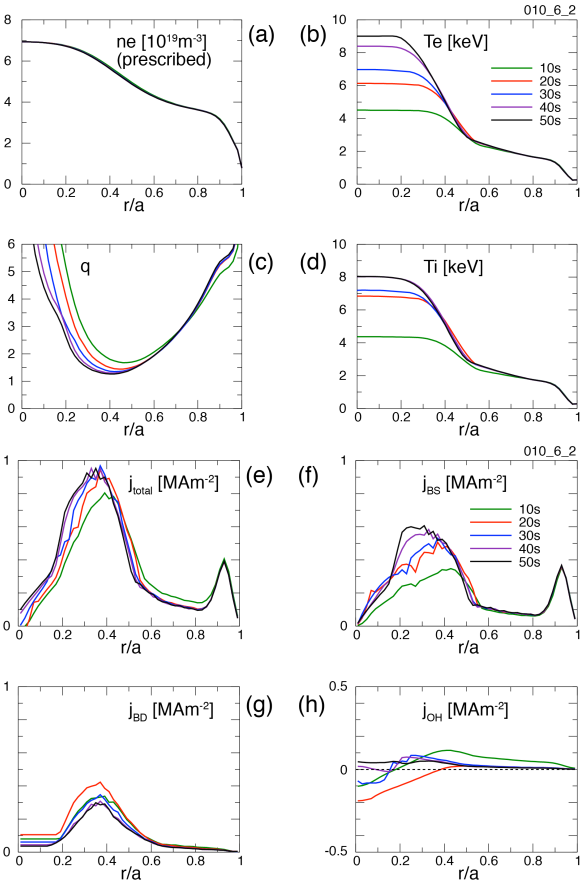

Fig. 3: Temporal evolutions of (a) prescribed ne profile, (b) T_e profile, (c) q profile, (d) T_i profile, (e) total current density, (f) bootstrap current density, (g) beam driven current density, (h) Ohmic current density, during the real-time control shown in Fig. 2.

density, β_N and V_{loop} are appropriately controlled at $\beta_N \geq 4$. Comparing two density regimes (Fig. 2 and 4), margins of both heating and CD power are wider in the low density, because CD efficiency is higher for higher T_e at lower density but the same β_N. Since N-NB (U) allocated for 0-5 MW power range is more off-axis than N-NB (L) for 5-10 MW (Fig. 1) and is mainly used at the low density, the location of minimum q in the low density is a little more outside than in the high density. The difference in q profile seems contributing the better confinement in the low density and improving the margin as well.

Without the V_{loop} control, V_{loop} becomes negative for both high and low density (Fig. 5 for low density). Then, recharge of poloidal magnetic field starts and PF coil currents eventually reach to their limits, which should be avoided in the steady-state operation.

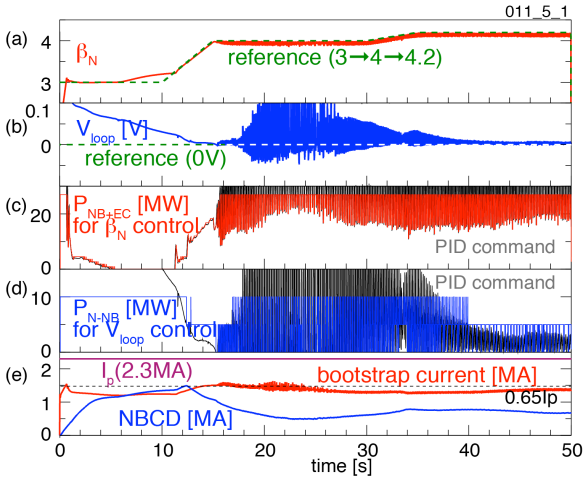

Fig. 4: Real-time control of β_N and V_{loop} at low density f_{GW}=0.52. (a) β_N and reference, (b) V_{loop} and reference, (c) P-NB and ECRF heating power controlling β_N, (d) N-NB current drive power controlling V_{loop}, (e) plasma current, bootstrap current and NBCD current.

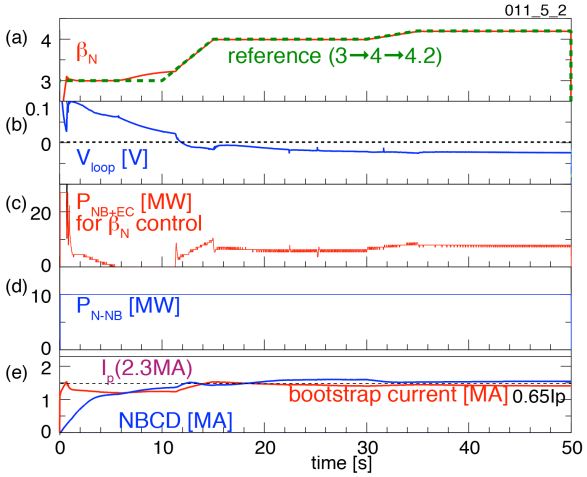

Fig. 5: Real-time control of sole β_N at low density f_{GW}=0.52: the same condition as Fig. 4, except V_{loop} not controlled. (a) β_N and reference, (b) V_{loop}, (c) P-NB and ECRF heating power controlling β_N, (d) N-NB current drive power (pre-programed) (e) plasma current, bootstrap current and NBCD current. The loop voltage stays negative without V_{loop} control.

4. Summary

We have investigated steady-state high beta operation scenarios implementing real-time control of β_N and V_{loop} in the TOPICS code. Simultaneous control of β_N and V_{loop} is possible at $\beta_N \geq 4$ in either high (f_{GW}=0.88) or low (f_{GW}=0.52) density. Margin of control power is wider in the low density. V_{loop} control (with I_p control) is essential for the steady-state operation. In the end, we note that the β_N control developed here is also essential in magnetic equilibrium control in all operation scenarios in order to avoid loss of equilibrium control due to PF coil voltage saturation.

This work was supported by KAKENHI 23360416. TS thanks to Mr I. Kamata for his support on programing the TOPICS code.

References

[1] Y. Kamada *et al.*, 24th IAEA FEC, San Diego 2012 OV4/1.

[2] S. Ide *et al.*, 24th IAEA FEC, San Diego 2012 FTP/P7-22.

[3] A. Fukuyama *et al.*, Plasma Phys. Control. Fusion **37** (1995) 611.